Materials Transactions, JIM, Vol. 39, No. 5 (1998), pp. 557 to 561

Evaluation of Anisotropic Lattice Strain of Co_9Fe/Cu Superlattice by Grazing Incidence X-ray Scattering Method

S. Sato*†, M. Saito*, E. Matsubara**,
Y. Waseda* and K. Inomata***

*Institute for Advanced Materials Processing, Tohoku University, Sendai 980-8577, Japan
**Department of Materials Science and Engineering, Graduate School, Kyoto University, Kyoto 606-8317, Japan
***Toshiba Corporation, Research and Development Center, Kawasaki 210-0901, Japan

Two different X-ray scattering experiments of θ-2θ X-ray scattering and grazing incidence X-ray scattering (GIXS) geometries have been done for evaluating the lattice strain anisotropically formed in the Co_9Fe/Cu superlattices. The magnitude of lattice strain along Cu [001] and [110] directions which are parallel to the surface was estimated using GIXS geometry. The results confirm that the lattice strain along both directions increases with decreasing Cu thickness and its degree changes with a variation in orientation. On the other hand, the magnitude of lattice strain along two directions of Cu [110] (parallel to the surface) and Cu [1$\bar{1}$0] (perpendicular to the surface) is found to differ from each other by comparing the lattice strain estimated from the measurements for equivalent Cu 220 reflections. The present results clearly suggest that the lattice strain formed in the Co_9Fe/Cu superlattices depends upon the lattice orientation.

(Received November 18, 1997; In Final Form February 5, 1998)

Keywords: *grazing incidence X-ray scattering, θ-2θ X-ray scattering, giant magnetoresistance, superlattice, lattice strain*

I. Introduction

Recently, novel devices utilizing the unique properties of superlattices have been stimulating a great interest from the fundamental and technological viewpoints. A soft X-ray monochromator is one of the well-known applications. In this case, the elements with low and large atomic numbers, such as, Si and W, are alternately stacked with a certain periodic thickness for obtaining an effective scattering power. A magnetic multilayer is one of the new applications of superlattices. In particular, the giant magnetoresistance (hereafter, referred to as GMR) has been intensively studied. In Co/Cu multilayers, for example, magnetoresistance ratios have been reported to be as large as 78% at 4.2 K and 48% at room temperature[1][2]. In addition to the GMR these multilayers show the antiferro- and ferro-magnetic oscillating behavior with increasing thickness of the layers of non-magnetic component[1][2]. Although such interesting properties of new synthetic materials are strongly affected by the atomic arrangement in layers, the origin of these peculiar features of multilayers are not well identified yet. This atomic arrangement is affected, more or less, by the strain formed in the stacked layers. Accordingly, accurate evaluation of the strain in superlattices is essential for characterizing their properties.

The conventional reflection geometry of θ-2θ X-ray scattering (see Fig. 1(a)) is widely used for characterizing the structure of a multilayer. Diffraction peaks provide us information about the strain, the orientational disorder of mosaic spread of the crystal and the thickness of individual layers. However, the structural information

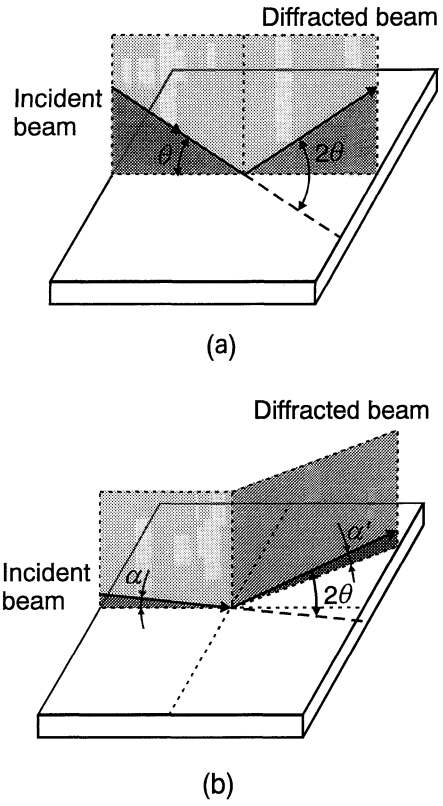

Fig. 1 Schematic diagram of X-ray scattering geometries. (a) θ-2θ X-ray scattering geometry and (b) GIXS geometry.

† Graduate Student, Tohoku University.

obtained with the θ-2θ X-ray scattering method alone is still far from complete, because the resultant structural information is limited to be one-dimensional.

The grazing incidence X-ray scattering (hereafter, referred to as GIXS) method, which was first developed by Marra *et al.*[3], has been often applied to characterize the structures of the surface, interface and thin films[4]-[8]. In the GIXS geometry (see Fig. 1(b)), monochromatic X-ray is incident on the surface at grazing angles less than or equal to a critical angle of total reflection, and scattering X-ray is detected in the in-plane direction. Thus, the scattering vector of the GIXS geometry is perpendicular to that of the θ-2θ X-ray scattering case. In addition to the geometrical difference from the θ-2θ X-ray scattering method, the GIXS method enables us to measure X-ray scattering sensitive to surface by using the feature of the X-ray total external-reflection phenomenon, which makes the X-ray penetration depth to the surface of materials shallow (typically from a few nm to several hundred nm).

The purpose of this work is to estimate the lattice strain anisotropically formed in the Co_9Fe/Cu superlattices by applying the GIXS method coupled with conventional θ-2θ X-ray scattering geometry in order to investigate the effect of orientation on the strain.

II. Experimental

A Co_9Fe/Cu multilayer set was deposited by ion beam sputtering on the MgO (110) single crystal substrate with different periodic lengths: (1) (Co_9Fe (1.0 nm)/Cu (0.8 nm))$_{16}$, (2) (Co_9Fe (1.0 nm)/Cu (2.0 nm))$_{16}$ and (3) (Co_9Fe (1.0 nm)/Cu (3.2 nm))$_{16}$. The base pressure was 5×10^{-5} Pa and sputtering was carried out using 1.3×10^{-2} Pa Ar ions. The details of the GMR properties of these multilayers are described elsewhere[9].

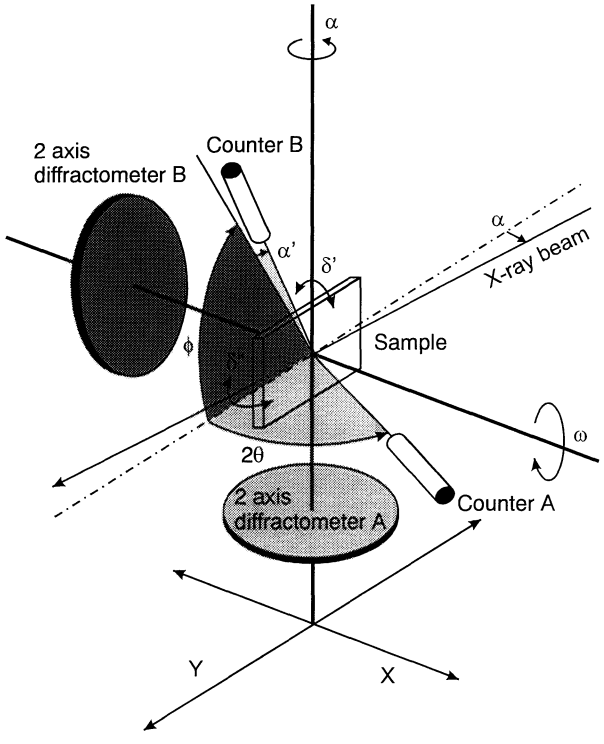

Fig. 2 Schematic diagram of configurations of rotation axes equipped with the crossed double-axis diffractometer used in this work.

The arrangement of the rotation axes of this diffractometer is explained in Fig. 2. The diffractometer is composed of two double-axis diffractometers. The diffractometer B, which is used for GIXS measurement, is vertically placed on the diffractometer A, which is used for θ-2θ X-ray scattering measurement. The rotation axes of both the diffractometers vertically intersect at the center of the sample surface. The scintillation counters are used for both the θ-2θ X-ray scattering and the GIXS measurements. Monochromatic Cu Kα radiation ($\lambda = 0.1542$ nm) was obtained from a Ge 111 single crystal using the rotating anode X-ray generator (Rigaku RU-300) with a copper target. A variety of different Bragg reflections of both Cu and Co_9Fe were studied with this apparatus.

III. Results and Discussion

1. X-ray reflectivity measurement

Figure 3 shows X-ray reflectivity curves, which were measured by the coupling scan of α and 2θ ($=2\alpha$) in Fig. 2, of Co_9Fe (1.0 nm)/Cu (0.8 nm), Co_9Fe (1.0 nm)/Cu (2.0 nm) and Co_9Fe (1.0 nm)/Cu (3.2 nm) multilayers, respectively. The critical angle of the total reflection of all multilayers appears at 6.91 mrad, as exemplified in Fig. 3(a). Thus, the incident angle α in the GIXS measurement was determined at this angle. Furthermore, these curves clearly show periodic oscillations, which should be attributed to the interference of the beams reflected by the specimen surface and interfaces. Then the periodic length of each layer in the Co_9Fe/Cu superlattice, which is estimated in the deposition process, has been well confirmed by comparing the period of oscillations of the experimental curves with those of calculated values using formula proposed by Parratt[10]. It is rather stressed here that the periodicity is a key factor in this comparison. In other words, the agreement in the absolute scale between calculation and the experimental reflectivity curve is out of scope.

2. Lattice strain in Cu layers

The orientation of the Cu layers is as follows: the orientation perpendicular to the surface is [1$\bar{1}$0], and the basal plane contains [001] and [110] directions. The lattice strain formed in the basal plane was at first evaluated for obtaining the orientational effect of [001] and [110]. Next, the strain formed in both the basal plane and this perpendicular plane was evaluated in order to survey the effect of these directions on strain.

Figure 4 shows the Cu 200 reflections of the Co_9Fe/Cu multilayers measured with the GIXS geometry along the Cu [001] direction. The peak intensity is normalized to unity. With decreasing thickness of Cu layers from 3.2 nm to 0.8 nm, the peaks is found to shift to higher angles

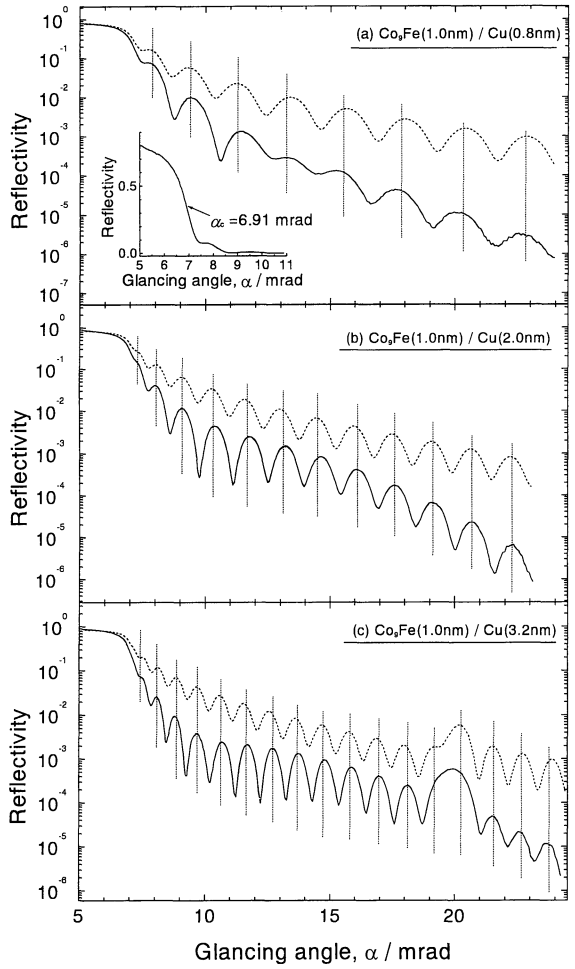

Fig. 3 Experimental X-ray reflection curves (solid lines) and calculated curves (broken lines) of (a) Co_9Fe (1.0 nm)/Cu (0.8 nm) (b) Co_9Fe (1.0 nm)/Cu (2.0 nm) (c) Co_9Fe (1.0 nm)/Cu (3.2 nm) multilayers, respectively.

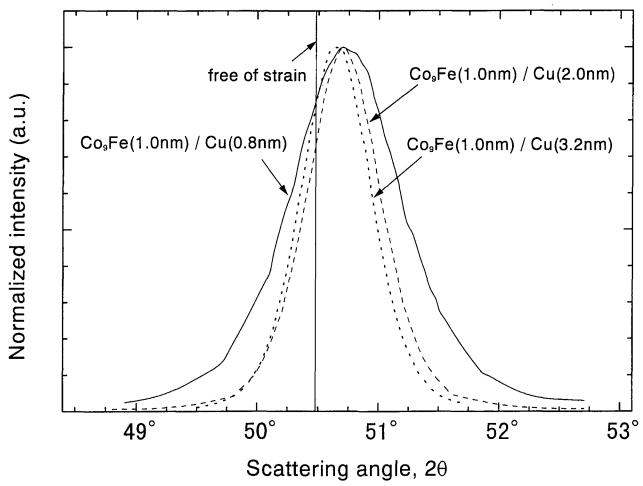

Fig. 4 Cu 200 reflections measured for Co_9Fe/Cu superlattice with GIXS geometry. Solid, broken and dotted lines represent the results of Co_9Fe (1.0 nm)/Cu (0.8 nm), Co_9Fe (1.0 nm)/Cu (2.0 nm) and Co_9Fe (1.0 nm)/Cu (3.2 nm) multilayers, respectively.

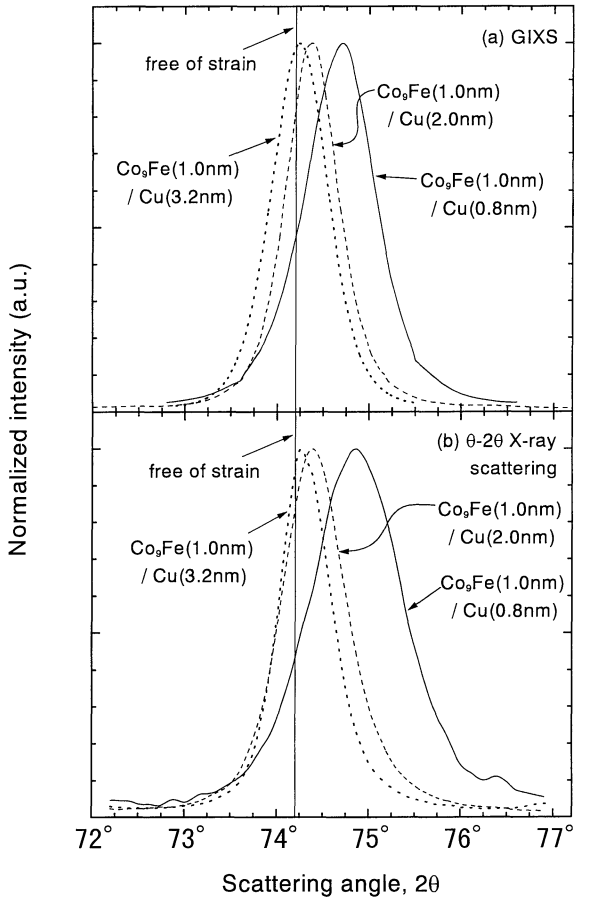

Fig. 5 Cu 220 reflections measured for Co_9Fe/Cu superlattice with (a) GIXS geometry and (b) θ-2θ X-ray scattering geometry. Solid, broken and dotted lines represent the results of Co_9Fe (1.0 nm)/Cu (0.8 nm), Co_9Fe (1.0 nm)/Cu (2.0 nm) and Co_9Fe (1.0 nm)/Cu (3.2 nm) multilayers, respectively.

away from the reference angular position (2θ=50.478°) given in the JCPDS (Joint Committee on Powder Diffraction Standards) card. The peak shift toward higher angles is due to contraction of Cu lattice along the interplanar [001] direction. Therefore, we can see that the contraction of Cu lattice is larger for thinner Cu layers. Furthermore, the full width at half maximum (FWHM) of the peak of Co_9Fe (1.0 nm)/Cu (0.8 nm) multilayer appears to be wider than the other peaks. This peak broadening is probably due to the inherent disorder of the Cu lattice. This disorder comes from the orientation disorder of mosaic spread of the Cu crystal, which is mainly attributed to the small thickness of Cu layers.

Figure 5(a) shows the Cu 220 reflections measured with the GIXS geometry along the Cu [110] direction. The peaks in all cases are detected at higher angles than the reference angular position (2θ=74.20°) given in the JCPDS card. As mentioned above, such peak shift is also due to the lattice contraction. Hence, the Cu lattice contraction along the Cu [110] direction is quite realistic. Furthermore, the peak shape of the 220 reflection for Co_9Fe (1.0 nm)/Cu (0.8 nm) is different from those for other two multilayers with respect to FWHM of the peak. This is ascribed to the texture of Cu layers, that is, the orientation disorder of mosaic spread of crystal.

The peak shift with decreasing Cu thickness observed in the 220 reflections differs from that observed in the 200 reflections. This difference is partly brought by the difference of sensitivity to strain between these two indices. However, the peak shift of Co_9Fe (1.0 nm)/Cu (0.8 nm) for the 220 reflection is quite distinct in comparison with other samples, while this inclination cannot be well recognized in the case of the 200 reflection. Thus, it may safely be said that the degree of lattice strain depends on the lattice orientation of Cu. For this reason, it is more appropriate to use equivalent reflections, *i.e.* Cu 220 reflections in this case, for comparing lattice strain formed along the direction parallel to surface with strain formed along the direction perpendicular to the surface (hereafter, referred to as perpendicular lattice strain).

Figure 5(b) shows the Cu 220 reflections in the [1$\bar{1}$0] direction perpendicular to surface using the θ-2θ X-ray scattering geometry for estimating the perpendicular lattice strain. It is worth mentioning that the peaks of the results in Fig. 5(b) are located at higher angles than those shown in Fig. 5(a) for all the three samples. Thus, the Cu lattice contraction perpendicular to the surface is suggested to be larger than the parallel case. It should be stressed that such a relationship is not true for all types of superlattices. However, the lattice orientation of Cu is one of the important factors in discussing the lattice strain in superlattices.

The lattice strain, ε, is defined by the following equation;

$$\varepsilon=\frac{a_{exp}-a_0}{a_0}$$

where a_{exp} and a_0 represent the lattice constant given by experimental values and the JCPDS card, respectively. According to this equation, the lattice strains estimated from the present results of Figs. 4 and 5 are summarized in Table 1. Again, we could conclude from these results that the lattice strain in the Co_9Fe/Cu superlattice clearly shows anisotropy, which depends on the lattice orientation of Cu. Moreover, from the result of Table 1, it is found that the volume of the Cu lattice shrinks at the rate from 0.49 to 1.79% with decreasing Cu thickness. Hence, it can safely be said that the thickness of layer is one of the important factors for determining the lattice volume. The coupling measurement of two geometries presented in this paper enables us to estimate the change of the lattice volume of thin films, whereas it is difficult to determine such change by the conventional method alone.

Table 1 The lattice strain (%) estimated from Cu 200 and 220 reflections.

Cu thickness (nm)	[001] Parallel to surface	[110] Parallel to surface	[1$\bar{1}$0] Normal to surface
0.8	−0.44	−0.59	−0.77
2.0	−0.40	−0.20	−0.24
3.2	−0.29	−0.06	−0.14

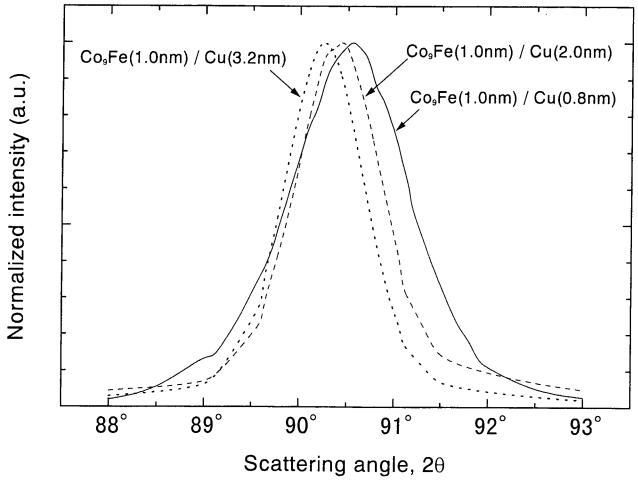

Fig. 6 X-ray scattering peaks measured for Co_9Fe/Cu superlattice with GIXS geometry. Solid, broken and dotted lines represent the results of Co_9Fe (1.0 nm)/Cu (0.8 nm), Co_9Fe (1.0 nm)/Cu (2.0 nm) and Co_9Fe (1.0 nm)/Cu (3.2 nm) multilayers, respectively.

3. Lattice strain in Co_9Fe layers

The diffraction peaks from the Co_9Fe layers were also investigated in the positions of hcp-Co 20$\bar{2}$0 and 0001 reflections by two geometries of GIXS and θ-2θ X-ray scattering, respectively. However, the peak around the hcp-Co 20$\bar{2}$0 reflection could not confirm a typical hexagonal symmetry when rotating the sample around its *c*-axis. Thus, the structure of Co_9Fe layers in this superlattice is considered not to be hcp-Co, and then it is difficult to discuss the structure of Co_9Fe layers in detail from the present results alone. For this reason, only the shift of Co_9Fe peaks accompanied with the variation in thickness of Cu layers was qualitatively analyzed.

Figure 6 shows the peaks detected around the hcp-Co 20$\bar{2}$0 reflection using GIXS geometry. In spite of a constant thickness value of 1.0 nm for Co_9Fe layers in all the samples, the peak positions in Fig. 6 are clearly found to shift to higher angles with decreasing thickness of Cu layers. This result indicates that the lattice strain of Co_9Fe layers depends on the thickness of Cu layers, which may be induced by disorder of Cu epitaxial layers.

IV. Concluding Remarks

The lattice strain anisotropically formed in the Co_9Fe/Cu superlattices has been estimated from θ-2θ X-ray scattering and GIXS geometries. The results are summarized as follows.

(1) The magnitude of the lattice strain along both the Cu [001] and [110] directions which are parallel to the surface increases with decreasing thickness of Cu layer suggesting that the degree of lattice strain changes with the variation in orientation.

(2) The detailed structure of the Co_9Fe layers could not be well-recognized in this study alone. Nevertheless, it could be safely concluded that the lattice strain in the basal plane was anisotropically formed depending on the

orientation of the Cu layers.

(3) The magnitude of lattice strain formed in the directions along the Cu [110] and Cu [1$\bar{1}$0] directions is found to differ from each other by comparing the lattice strain estimated from the measurements of equivalent Cu 220 reflections. This suggests that the lattice strain formed in the Co_9Fe/Cu superlattices is affected by the lattice orientation.

Our results show that the lattice parameters of superlattices need to be determined by the combination of θ-2θ X-ray scattering and GIXS geometries, particularly for a detailed discussion including the lattice strain.

Acknowledgment

This research is supported by the Grant-in-Aid for Encouragement of Young Scientists (No. 09750727) from the Ministry of Education, Science, Sports and Culture of Japan.

REFERENCES

(1) D. H. Mosca, F. Petroff, A. Fert, P. A. Schroeder, W. P. Pratt, Jr., R. Laloee and S. Lequien: J. Magn. & Magn. Mater., **94** (1991), L1.
(2) S. S. P. Parkin, R. Bhadra and K. P. Roche: Phys. Rev. Lett., **66** (1991), 2152.
(3) W. C. Marra, P. Eisenberger and A. Y. Cho: J. Appl. Phys., **50** (1979), 6927.
(4) J. Bohr, R. Feidenhans'l, M. Tonry, R. L. Johnson and I. K. Robinson: Phys. Rev. Lett., **54** (1985), 1275.
(5) K. Akimoto, K.Hirose and J. Mizuki: Phys. Rev., **B44** (1991), 1622.
(6) D. Bohr, W. Press, R.Jebasinski and S. Mantal: Phys. Rev., **B47** (1993), 4385.
(7) R. A. Cowley and T. W. Ryan: J. Phys. D: Appl. Phys., **20** (1980), 16.
(8) M. Saito, T. Kosaka, E. Matsubara and Y. Waseda: Mater. Trans., JIM, **36** (1996), 1.
(9) K. Inomata, Y. Saito and S. Hashimoto: J. Magn. Magn. Mater., **121** (1993), 350.
(10) L. G. Parratt: Phys. Rev., **95** (1954), 359.